LARAM School 2008 (7-22 September, Ravello, Italy)

SESSION 1: Landslide analysis using approaches based on: Geology, Geotechnics and Geomechanics

Basic Geodynamics of Landslides

III. Flow-slides

Ioannis Vardoulakis

National Technical University of Athens

September 2008

http://geolab.mechan.ntua.gr/, I.Vardoulakis@mechan.ntua.gr

III. Flow-slides

1 1-D "Shallow-water" equations for flow-slides

1.1 General formulation

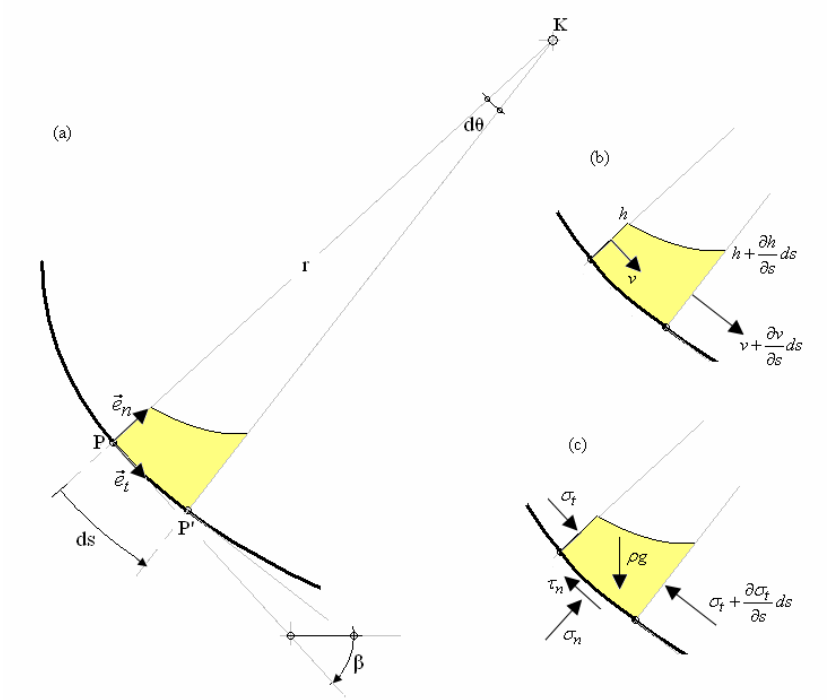

Figure 1-1: Debris element on a curved track. a) Local coordinate system. b) Flow variables, velocity and height. c) tractions on element

The last two phases of the evolution of a catastrophic landslide are its flow- and deposition. Here we consider slides that are "long" in the direction normal to the main flow plane. The corresponding mathematical theory is an 1-D, "shallow-water" approximation of flow-slide motion on a track with variable topography (Savage & Hutter [7], Figure 1-1 (a)). The position of any point P of the track is given by the arc-length coordinate s. The track is approximated locally by its circle of curvature $K(r)$. Thus, at any point $P(s)$ of the track we introduce the local coordinate system $P(\vec{e}_t, \vec{e}_n)$ with ortho-normal base vectors, tangential and normal to the track at this point. At any time t at a point $P(s)$ we define the flow-height as a function of position and time (Eulerian description),

$$h = h(s,t) \tag{1.1}$$

The width of this section length perpendicular to the considered plane is computed from the total "wet" surface area of the normal section at the considered position

$$b = \frac{A}{h} \tag{1.2}$$

Accordingly the cross-sectional flow velocity is defined as,

$$v = \frac{q}{A} = v(s,t) \tag{1.3}$$

where q is the total volumetric flow across the considered normal section.

The flow velocity is taken tangential and is assumed to be a function of position and time only,

$$\vec{v} = v\vec{e}_t \tag{1.4}$$

The acceleration has however a tangential and a normal component,

$$\vec{a} = a_t\vec{e}_t + a_n\vec{e}_n \tag{1.5}$$

where,

$$a_t = \dot{v} \tag{1.6}$$

is the "material" time derivative of the velocity (see Appendix II, Sect. 5),

$$\dot{v} = \frac{\partial v}{\partial t} + v\frac{\partial v}{\partial s} \tag{1.7}$$

and

$$a_n = \frac{v^2}{r} \tag{1.8}$$

is the centripetal acceleration.

Mass balance for the considered flow element (Figure 1-1 (b)) yields,

$$\frac{\partial h}{\partial t} + \frac{\partial}{\partial s}(hv) = 0 \tag{1.9}$$

Momentum balance in normal directions reads,

$$\nearrow: \quad \sigma_n ds - \rho g \cos\beta h ds - \sigma_t h d\theta = \rho h ds \frac{v^2}{r}$$

or

$$\sigma_n = \rho g \cos\beta h + \frac{h}{r}\left(\sigma_t + \rho v^2\right) \tag{1.10}$$

In eq. (1.10) with β we denote the local inclination angle of the track with respect to the horizontal direction (Figure 1-1 (a)).

We assume that the lateral pressure is proportional to the basal normal reaction,

$$\sigma_t = K\sigma_n \tag{1.11}$$

Let φ' be the internal friction coefficient of the material. The lateral pressure coefficient usually is taken as

$$K = \begin{cases} 1 & if: \beta \geq \varphi' \\ K_a & if: 0 \leq \beta \leq \varphi' \quad and\ active\ plastic\ flow \\ K_p & if: 0 \leq \beta \leq \varphi' \quad and\ pasive\ plastic\ flow \end{cases} \tag{1.12}$$

where $K_{a/p}$ is the *active/passive earth-pressure coefficient* of limit analysis (see Appendix II, Sect. 6)

$$K_{a/p} = 2\left(1 \mp \sqrt{1 - \frac{\cos^2\varphi'}{\cos^2\beta}}\right)\frac{1}{\cos^2\varphi'} - 1 \tag{1.13}$$

Notice that for,

$$\beta = \varphi' - \delta \quad , \quad 0 \leq \delta << 1 \tag{1.14}$$

$$K_{p/a} = \frac{1 + \sin^2\varphi'}{\cos^2\varphi'} \pm O\left(\delta^{1/2}\right) \tag{1.15}$$

And if φ is small, then from eq. (1.15) we get,

$$K_{p/a} = 1 + \frac{1}{2}\varphi'^2 + O\left(\varphi'^4\right) \tag{1.16}$$

With this result we have a justification of the usually met assumption that $K=1$, for $\beta \geq \varphi'$, cf. eq. (1.12). This assumption could be replaced by the following (cf. eq.(1.15)),

$$K=\begin{cases} \left(1+\sin^2\varphi'\right)/\cos^2\varphi' & if:\beta \geq \varphi' \\ K_a \quad if:0\leq\beta\leq\varphi' & and\ active\ plastic\ flow \\ K_p \quad if:0\leq\beta\leq\varphi' & and\ pasive\ plastic\ flow \end{cases} \tag{1.17}$$

This means that always holds

$$K=O(1) \tag{1.18}$$

From eqs. (1.10) and (1.11) we get,

$$\sigma_n\left(1-K\frac{h}{r}\right)=\rho g h\cos\beta+\frac{h}{r}\rho v^2 \tag{1.19}$$

Let the normalized flow-height be,

$$h^*=\frac{h}{r} \tag{1.20}$$

Notice that $r\to\infty$ (planar track) the normalized flow-height $h^*\to 0$. In general we will assume that the normalized flow-height is small if compared the radius of curvature of the track, and

$$0\leq h^* << 1 \tag{1.21}$$

In this case from eqs. (1.18) to (1.21) we get,

$$\sigma_n=\rho h\left(g'+\frac{v^2}{r}\right)+K\rho g' h h^*+O(h^{*2})$$

or

$$\sigma_n\approx\rho h\left(g'+\frac{v^2}{r}\right) \tag{1.22}$$

where

$$g' = g\cos\beta \tag{1.23}$$

In eq. (1.22) we recognize the first term as the static basal reaction and the second term as the dynamic (centripetal) basal reaction.

Balance of linear momentum in tangential direction yields,

$$\searrow: \quad -\frac{\partial}{\partial s}\left(h\sigma_t\right) + \rho g h \sin\beta - \tau_n = \rho h \dot{v} \tag{1.24}$$

In most cases we will assume that the shear reaction is purely frictional and that the basal (Coulomb) friction is equal to internal friction,

$$\tau_n = \sigma_n \tan\varphi \tag{1.25}$$

With these assumptions from eqs. (1.22) to (1.25) we get,

$$\frac{\partial v}{\partial t} + v\frac{\partial v}{\partial s} + \frac{1}{h}\frac{\partial}{\partial s}\left(Kg'h^2\left(1+\frac{1}{g'}\frac{v^2}{r}\right)\right) = g'\left(\tan\beta - \tan\varphi\left(1+\frac{1}{g'}\frac{v^2}{r}\right)\right) \tag{1.26}$$

Eqs. (1.9) and (1.26) constitute the set of governing partial differential equations of flow-slides in an 1D-setting and variable topography. They are usually termed as "shallow-water" equations or "depth-integrated" equations. They constitute a system of quasi-linear hyperbolic p.d. eqs. The solutions of these equations include the formation of sharp discontinuities ("shocks"; see Sect. 3), thus such a system of hyperbolic equations is treated numerically by the so-called "shock capturing" techniques. In that respect we refer here to a remark made by Gray et al. [4]; see references therein and Tai et al. [9]): *" …The development of these methods has a long history starting with the classic papers of Godunov (1959), Van Leer (1979), Harten (1983) and Yee (1987), and there are now a wide range of textbooks on the subject (e.g. Le Veque 1990; Godlewski & Raviart 1996; Kröner 1997; Toro 1997). Here we have opted to use the recent high-resolution shock-capturing non-oscillatory central (NOC) scheme first introduced by Nessyahu & Tadmor (1990) and extended to multi-dimensions by Arminjon & Viallon (1995, 1999); Jiang & Tadmor (1998) and Lie & Noelle (2003)…"*. Recently Professor M. Pastor and his team have developed a 2D-model for the analysis of the propagation of fast landslides, using a Finite Element Method and the Navier–Stokes depth-integrated equations.

1.2 The circular track

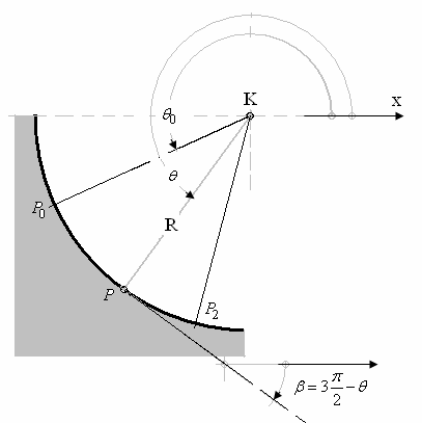

Figure 1-2: Circular track

As an application of the set of governing eqs. (1.9) and (1.26) we consider the case of a circular track. Notably that in Geotechnics one usually approximates the "failure surface" with a section of a circular cylinder, ; c.f. $K(R)$ [11]. In this particular case, as shown in Figure 1-2, we have that

$$r = R = const. \quad , \quad ds = Rd\theta \tag{1.27}$$

and

$$\beta = 3\frac{\pi}{2} - \theta \tag{1.28}$$

Eq. (1.23) reads,

$$g' = -g\sin\theta \tag{1.29}$$

and with that the momentum balance eq. (1.26) becomes,

$$\begin{aligned} &\frac{\partial v}{\partial t} + \frac{v}{R}\frac{\partial v}{\partial \theta} + \frac{g}{hR}\frac{\partial}{\partial \theta}\left(Kh^2\left(-\sin\theta + \frac{1}{g}\frac{v^2}{R}\right)\right) \\ &= -g\sin\theta\left(\cot\theta - \tan\varphi\right) - \tan\varphi\frac{v^2}{R} \end{aligned} \tag{1.30}$$

We introduce the following set of non-dimensional independent and dependent variables,

$$\theta^* = \theta \quad , \quad t^* = \frac{t}{\sqrt{\frac{R}{g}}}$$
$$v^* = \frac{v}{\sqrt{gR}} \quad , \quad h^* = \frac{h}{R} \tag{1.31}$$

In terms of dimensionless variables the governing mass- and momentum balance eqs. (1.9) and (1.30) become,

$$\frac{\partial h}{\partial t} + \frac{\partial}{\partial \theta}(hv) = 0 \tag{1.32}$$

$$\frac{\partial v}{\partial t} + v\frac{\partial v}{\partial \theta} + \frac{1}{h}\frac{\partial}{\partial \theta}\left(Kh^2\left(-\sin\theta + v^2\right)\right) = -\sin\theta\left(\cot\theta - \tan\varphi\right) - v^2\tan\varphi \tag{1.33}$$

where for simplicity in notation we omitted the superimposed asterix*.

Notice that the forcing term on the r.h.s. of eq. (1.33) expressed in terms of the sloping angle β of the circular track takes the following form,

$$b = \sin\beta - \left(\cos\beta + v^2\right)\tan\varphi \tag{1.34}$$

From this expression it becomes clear that the curved topography induces an additional resistance to flow due to the development of centripetal forces, which for a dry material result in an increase of the frictional (resisting) forces. These forces are proportional to v^2 and are important in rapid flow regimes.

2 Steadily moving mud-flow down on a planar track

For a planar track we have that,

$$s \equiv x \quad , \quad \beta = const. \quad , \quad 1/r = 0 \tag{2.1}$$

In that case the governing equations become,

$$\frac{\partial h}{\partial t} + \frac{\partial}{\partial x}(hv) = 0 \tag{2.2}$$

$$\frac{\partial v}{\partial t}+v\frac{\partial v}{\partial x}+\frac{1}{h}\frac{\partial}{\partial x}\left(Kg'h^2\right)=g'\left(\tan\beta-\frac{\tau_n}{\sigma_n}\right) \tag{2.3}$$

As an application of these equations we consider here a mudflow-slide, moving on a planar track (cf. Figure 2-1).

Figure 2-1: An aerial view shows Saturday, Feb. 18, 2006, the extent of the landslide that buried the whole village of Guinsaugon, St. Bernard town in Southern Leyte province in central Philippines. Officials estimate those who perished in the landslide to be 1,800. [AP]

In order to model the mud-flow we assume that the basal friction obeys a Bagnold [1] rheology. Accordingly for fast shear flows of muddy soils we assume that instead of eq. (1.25) the following friction law holds

$$\tau_n=\sigma_n'\tan\varphi+f\sqrt{\nu_w}\dot{\gamma}^n \quad , \quad n=3/2 \tag{2.4}$$

where σ_n' denotes the basal Terzaghi-effective stress,

$$\sigma_n'=\rho' hg' \quad , \quad \rho'=\rho-\rho_w \tag{2.5}$$

where ρ_w is the density of water. With ν_w we denote the kinematic viscosity of water.

According to Bagnold for fast shear flows of clayey materials the coefficient f has the following structure

$$f\approx 0.26\lambda_B^{7/4}\sqrt{\rho_w\rho_s}\,D_g \tag{2.6}$$

The factor λ_B depends on the porosity of the mixture,

$$\lambda_B = \frac{1}{\left(\frac{1-n_{\min}}{1-n}\right)^{1/3} - 1} \tag{2.7}$$

and D_g is here the mean particle size.

Mudflows are considered to be shear-flows, thus in eq. (2.4) $\dot{\gamma}$ is replaced here by the mean shear-rate (see Apendix III, Sect. 7),

$$\dot{\gamma} \approx 2\frac{v}{h} \tag{2.8}$$

The factor 2 in eq. (2.8) is because v a mean flow velocity. With these assumptions the governing momentum eq. (2.3) becomes,

$$\frac{\partial v}{\partial t} + v\frac{\partial v}{\partial x} + \frac{1}{h}\frac{\partial}{\partial x}\left(Kg'h^2\right) = g'\left(\tan\beta - \frac{\rho'}{\rho}\tan\varphi' - 2^{3/2}\,\frac{f\sqrt{v_w}}{\rho g' h}\left(\frac{v}{h}\right)^{3/2}\right) \tag{2.9}$$

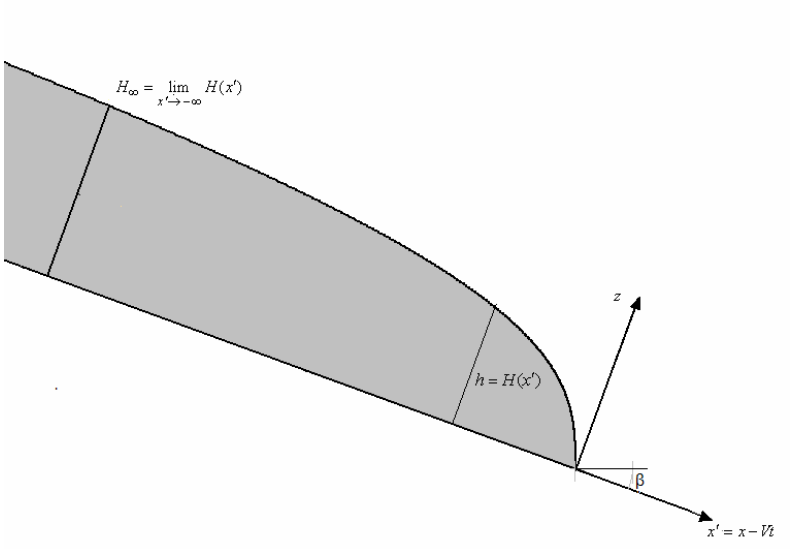

Figure 2-2: Steadily moving mudslide

In order to investigate further the above set of governing equations we consider the case of steadily moving mudslide with speed [8],

$$v = V = const. \quad \Rightarrow \quad \dot{v} = \frac{\partial v}{\partial t} + v\frac{\partial v}{\partial x} = 0 \tag{2.10}$$

In that case we assume that the profile of the moving body is constant; i.e. with the aid of a steadily moving coordinate system,

$$x' = x - Vt \quad , \quad V = const. \tag{2.11}$$

We assume that

$$h = H(x') \tag{2.12}$$

With this ansatz the mass balance equation (2.2) is satisfied identically, whereas the momentum balance equation (2.9) yields an equation for the moving flow-profile

$$2K\frac{dH}{dx'} = m - \mu'_{st} - \mu_{dn} \tag{2.13}$$

where m is the slope inclination that plays the role of the driving force (gravity):

$$m = \tan\beta \tag{2.14}$$

μ'_{st} is the Terzaghi-effective static friction:

$$\mu'_{st} = \frac{\rho'}{\rho}\tan\varphi \tag{2.15}$$

and μ_{dn} is the Bagnold-dynamic friction:

$$\mu_{dn} = cV^{3/2}H^{-5/2} \tag{2.16}$$

The constant c in eq. (2.16) is

$$c = 2^{3/2}\frac{f\sqrt{\nu_w}}{\rho g'} = 0.26\lambda_B^{7/4}\frac{\sqrt{\rho_w\rho_s}}{\rho}\frac{\sqrt{\nu_w}D_g}{g'} \tag{2.17}$$

This parameter has the dimensions

$$[c] = \frac{LT^{-1/2}L}{LT^{-2}} = LT^{3/2} \tag{2.18}$$

that cancel out the dimensions of remaining terms on the r.h.s. of eq. (2.16)

$$[V^{3/2}H^{-5/2}] = L^{3/2}T^{-3/2}L^{-5/2} = L^{-1}T^{-3/2} \tag{2.19}$$

Let the height of the mud-flow wave, at large distance from its front be denoted as,

$$H_\infty = \lim_{x' \to -\infty} H(x') \tag{2.20}$$

We assume that at this distance the flow height reaches its maximum,

$$\left.\frac{dH}{dx'}\right|_{x' \to -\infty} = 0 \tag{2.21}$$

Then from eq. (2.13) we get an expression for the velocity of the considered mud-flow wave:

$$0 = m - \mu'_{st} - cV^{3/2}H_\infty^{5/2} \quad \Rightarrow \quad V = \left(\frac{b}{c}\right)^{2/3} H_\infty^{5/3} \tag{2.22}$$

where

$$b = m - \mu'_{st} \tag{2.23}$$

Thus the Bagnold model predicts a higher than linear dependency of the velocity on the flow- height ($V \sim H_\infty^{5/3}$).

For a realistic application we must adjust the values of the various parameters that enter the above formula in order to get realistic predictions for the mud-flow velocity. In view of eq. (2.22) in the term,

$$b = \tan\beta - \frac{\rho'}{\rho}\tan\varphi \tag{2.24}$$

the density ratio is usually about

$$\frac{\rho'}{\rho} \approx \frac{1}{2} \tag{2.25}$$

Remark:

We recall from the static slope stability analysis that in case of an infinite slope under the action of seepage the safe slope inclination is ,

$$\tan\beta < \frac{\rho'}{\rho}\tan\varphi \approx \frac{1}{2}\tan\varphi \qquad (2.26)$$

which in practical terms is usually referred to as,

$$\beta < \frac{1}{2}\varphi \qquad (2.27)$$

The implication of this estimate are evident. If we have a natural slope that after a heavy and protracted rainfall gets water-saturated (e.g. due to loss of its protecting cover-vegetation…) then this slope will become unstable if the ineq. (2.26) does not hold. In that case we may have the triggering of the herein considered mud-flow.

If we assume for example that the slope has an mean inclination of $\beta = 10^\circ$ and that the internal friction of the remolded clay is about $\varphi \approx 5^\circ$, then, $b \approx 0.133$ and $c \approx 0.5m\sec^{3/2}$ With this input eq. (2.22) yields,

$$V \approx \lambda \cdot H_\infty^{5/3} \quad , \quad \lambda \approx 0.4\frac{1}{m^{2/3}\sec} \qquad (2.28)$$

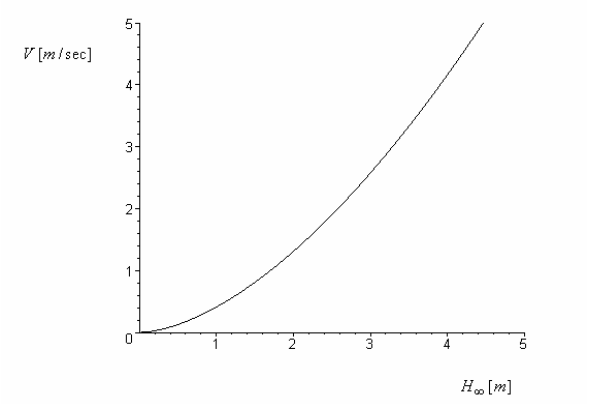

Figure 2-3: Calibration of the height-velocity eq. (2.22) for mud-flow on a gentle planar slope

As shown in Figure 2-3, the resulting speeds are of the order of a few meters per second.

With the above notation the governing eq. (2.13) becomes

$$\frac{dH}{dx'} = B\left(1-\left(\frac{H}{H_\infty}\right)^{-5/2}\right) \tag{2.29}$$

where

$$B = \frac{b}{2K} \tag{2.30}$$

With the change of variables

$$x^* = -\frac{x'}{H_\infty}\ ,\ h^* = \frac{H}{H_\infty} \tag{2.31}$$

eq. (2.29) becomes (Figure 2-2)

$$\frac{dh^*}{dx^*} = -B\left(1-h^{*-5/2}\right) \tag{2.32}$$

or

$$x^* = -\frac{1}{B}\int_0^{h^*}\frac{dy}{1-y^{-5/2}} \tag{2.33}$$

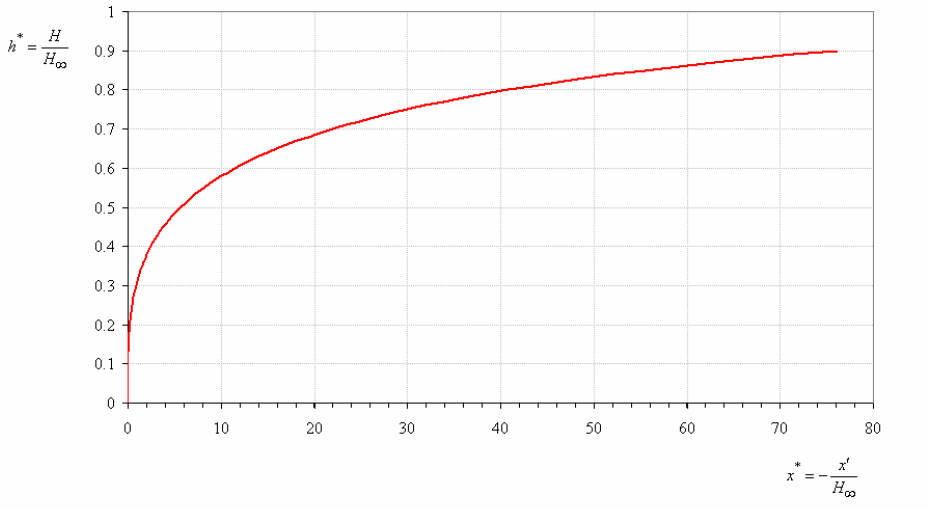

Figure 2-4: Profile of the mud-flow wave in terms of dimensionless variables

We notice that

$$-\frac{1}{1-y^{-5/2}} = y^{5/2} + y^5 + y^{15/2} + y^{10} + y^{25/2} + O\left(y^{15}\right) \tag{2.34}$$

and with that we get from eq.(2.33) (Figure 2-4),

$$x^* \approx \frac{1}{B}\left(\frac{2}{7}h^{*7/2} + \frac{1}{6}h^{*6} + \frac{2}{17}h^{*17/2} + \frac{1}{11}h^{*11} + \frac{2}{27}h^{*27/2} + \cdots\right) \tag{2.35}$$
$$for: \quad 0 \le h^* < 1$$

We observe that the Bagnold model predicts an infinite slope at the tip, since from eq. (2.35) we get (Figure 2-5

$$h^* \approx \frac{1}{2}\left(\frac{7}{2}Bx^*\right)^{2/7} \Rightarrow$$
$$\frac{dh^*}{dx^*} \approx B\left(\frac{2}{7}\frac{1}{\left(Bx^*\right)}\right)^{5/7} = O\left(x^{*-5/7}\right) \to \infty \quad for: x^* \to 0 \tag{2.36}$$

Such a profile will have severe impact on structures it may encounter on its way!

Figure 2-5: Photo of a debris flowexperiment, taken from R.M. Iverson, J.E. Costa, and R.G. LaHusen, 1992, Debris-Flow Flume at H.J. Andrews Experimental Forest, Oregon: U.S. Geological Survey Open-File Report 92-483. The flow-wave shows the formation of steep front and the development of roll-waves (http://vulcan.wr.usgs.gov/Projects/MassMovement/Publications/OFR92-483/OFR92-483_inlined.html)

3 The deposition bore

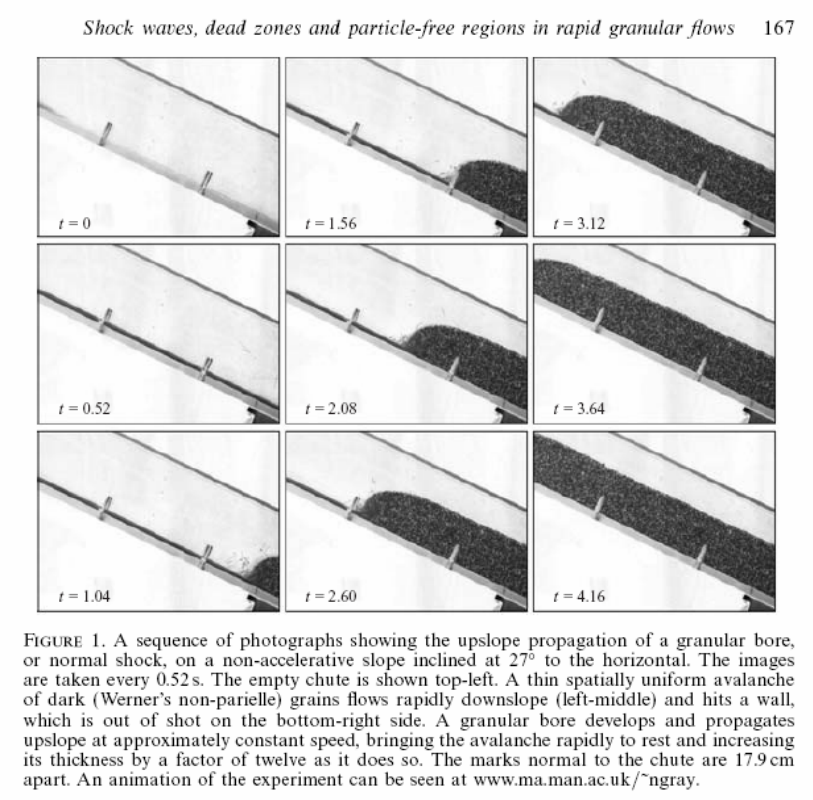

FIGURE 1. A sequence of photographs showing the upslope propagation of a granular bore, or normal shock, on a non-accelerative slope inclined at 27° to the horizontal. The images are taken every 0.52 s. The empty chute is shown top-left. A thin spatially uniform avalanche of dark (Werner's non-parielle) grains flows rapidly downslope (left-middle) and hits a wall, which is out of shot on the bottom-right side. A granular bore develops and propagates upslope at approximately constant speed, bringing the avalanche rapidly to rest and increasing its thickness by a factor of twelve as it does so. The marks normal to the chute are 17.9 cm apart. An animation of the experiment can be seen at www.ma.man.ac.uk/~ngray.

Figure 3-1: Granular bore after Gray et al.[4]

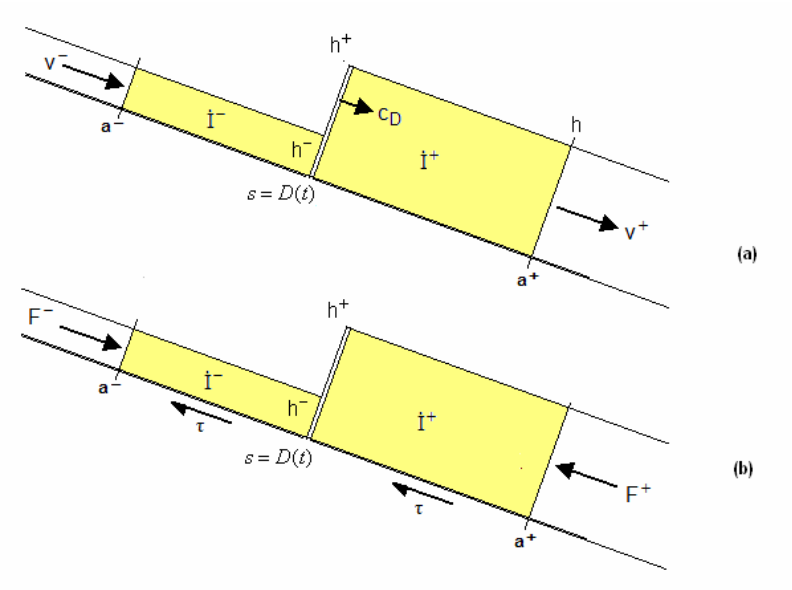

Figure 3-2: The moving shock, mass balance

As indicated in Figure 3-1, in order to capture discontinuous structures like an uphill moving deposition bore in debris flow we need to consider the possibility of a moving strong discontinuity. As is shown in Figure 3-2 the curvature of the track is neglected since all considerations are done in the tangential direction. At time t the discontinuity is at a position, $s = D(t)$. The discontinuity is moving with the speed,

$$c_D = \frac{dD}{dt} \tag{3.1}$$

Across this section the flow velocity, the flow-height, the flow-velocity and the discharge are discontinuous. Let the corresponding jumps be the difference between the right hand (dawn-stream) and left hand (up-stream) limits of the considered fields

$$[[h]] = h^+ - h^- \quad , \quad [[v]] = v^+ - v^- \quad , \quad [[q]] = v^+h^+ - v^-h^- \tag{3.2}$$

In order to formulate the compatibility conditions for these jumps we consider first the expression for the change of mass of segment of the flow-slide between the normal sections at the positions $x = a$ and $x = c$, and unit width:

$$\dot{m} = \int_a^c \frac{\partial}{\partial t}\left(\rho h\right) ds + v(c,t)\left(\rho h\right)_{s=c} - v(a,t)\left(\rho h\right)_{s=a} = 0 \tag{3.3}$$

We apply this result on both sides of a moving discontinuity section:

$$\begin{aligned} \dot{m}^- &= \int_{a^-}^{D(t)} \frac{\partial h}{\partial t} ds + c_D h^- - v(a^-,t)\, h(a^-,t) = 0 \\ \dot{m}^+ &= \int_{D(t)}^{a^+} \frac{\partial h}{\partial t} ds + v(a^+,t)\, h(a^+,t) - c_D h^+ = 0 \end{aligned} \tag{3.4}$$

Thus the total mass rate is

$$\dot{m} = \dot{m}^- + \dot{m}^+ = \int_{a^-}^{a^+} \frac{\partial h}{\partial t} ds + c_D h^- - v(a^-,t)h(a^-,t) + v(a^+,t)h(a^+,t) - c_D h^+ = 0 \tag{3.5}$$

We consider the limit of the above expression as, $a^- \to D(t)$, $a^+ \to D(t)$. For this limit the integrals in the above expression vanish and the remaining terms yield the *1st Rankine-Hugoniot* compatibility condition for the moving discontinuity section,

$$c_D h^- - v^- h^- + v^+ h^+ - c_D h^+ = 0 \quad \Rightarrow \quad c_D \left(h^+ - h^- \right) = v^+ h^+ - v^- h^- \tag{3.6}$$

or

$$c_D = \frac{[[q]]}{[[h]]} \tag{3.7}$$

Secondly we consider the total force and momentum in longitudinal direction of a segment of the flow-slide between the normal sections at the positions $x = a$ and $x = c$:

$$F = \frac{1}{2} K \rho g' h^2(a,t) - \frac{1}{2} K \rho g' h^2(c,t) + \int_a^c \tau ds \tag{3.8}$$

$$\mathrm{I} = \int_a^c \rho h v ds \tag{3.9}$$

The rate of longitudinal momentum is,

$$\dot{\mathrm{I}} = \int_a^c \rho \frac{\partial}{\partial t}(hv) ds + v(c,t)\left(\rho h v\right)_{s=c} - v(a,t)\left(\rho h v\right)_{s=a} \tag{3.10}$$

Balance of momentum requires that

$$L = F - \dot{\mathrm{I}} = 0 \tag{3.11}$$

where (Figure 3-2)

$$F = \frac{1}{2} K g' h^2(a^-,t) - \frac{1}{2} K \rho g' h^2(a^+,t) + \int_{a^-}^{a^+} \tau dx \tag{3.12}$$

and

$$\dot{I} = \dot{I}^- + \dot{I}^+ \tag{3.13}$$

Thus from

$$\dot{\mathrm{I}} = \int_{a^-}^{a^+} \rho \frac{\partial}{\partial t}(hv)ds + c_D\left(\rho hv\right)_{s=D^-} - v(a^-,t)\left(\rho hv\right)_{s=a^-} + v(a^+,t)\left(\rho hv\right)_{s=a^+} - c_D\left(\rho hv\right)_{s=a^+} \tag{3.14}$$

for the considered limits we get,

$$\begin{aligned} F &= \frac{1}{2}K^-\rho g'(h^-)^2 - \frac{1}{2}K^+\rho g'(h^+)^2 \\ \dot{\mathrm{I}} &= c_D\left(\rho hv\right)^- - v^-\left(\rho hv\right)^- + v^+\left(\rho hv\right)^+ - c_D\left(\rho hv\right)^+ \end{aligned} \tag{3.15}$$

From eqs. (3.13) and (3.15) we get *the 2nd Rankine-Hugoniot* compatibility condition for the moving discontinuity

$$\begin{aligned} &\frac{1}{2}K^-g'(h^-)^2 - \frac{1}{2}K^+g'(h^+)^2 = \\ &\quad c_D\left(hv\right)^- - v^-\left(hv\right)^- + v^+\left(hv\right)^+ - c_D\left(hv\right)^+ \end{aligned} \tag{3.16}$$

or

$$[[qv]] - c_D[[q]] = \frac{1}{2}[[Kg'h^2]] \tag{3.17}$$

Due to the 1st R.-H. condition, eq. (3.7), from eq. (3.17) we get,

$$[[qv]] - \frac{[[q]]^2}{[[h]]} = \frac{1}{2}[[Kg'h^2]] \tag{3.18}$$

We remark that the existence or not of base friction terms does not affect the 2nd Rankine-Hugoniot compatibility conditions.

Based on the above compatibility conditions we may return to the consideration of an uphill moving deposition bore. We assume that the velocity of the material behind the deposition bore is zero,

$$v^+ = 0 \tag{3.19}$$

Thus from eqs. (3.6) and (3.16) we get

$$c_D\left(h^+ - h^-\right) = -v^- h^- \tag{3.20}$$

$$\frac{1}{2}K^- g'(h^-)^2 - \frac{1}{2}K^+ g'(h^+)^2 = \quad c_D\left(hv\right)^- - v^-\left(hv\right)^- \tag{3.21}$$

The solution of these conditions is

$$c_D = -\sqrt{g'\frac{h^-}{h^+}\frac{K^+h^{+2} - K^-h^{-2}}{2\left(h^+ - h^-\right)}} \tag{3.22}$$

The minus sign in eq. (3.22) means that the bore is moving up-hill.

The deposition bore is observed at slope inclinations where uniform flow is possible. For the simple of Coulomb type friction law this is the case when

$$\beta = \varphi \tag{3.23}$$

Accordingly we assume that (see Sect. 6)

$$K^+ = K^- = \frac{1+\sin^2\varphi}{\cos^2\varphi} \tag{3.24}$$

and with that from eq. (3.22) we get (Gray et al. [4])

$$c_D = -\lambda\sqrt{g\bar{h}} \tag{3.25}$$

where

$$\bar{h} = \frac{1}{2}\left(h^+ + h^-\right) \tag{3.26}$$

and

$$\lambda = \sqrt{\cos\varphi\frac{1+\sin^2\varphi}{\cos^2\varphi}}\sqrt{\frac{h^-}{h^+}} \tag{3.27}$$

4 Roll waves

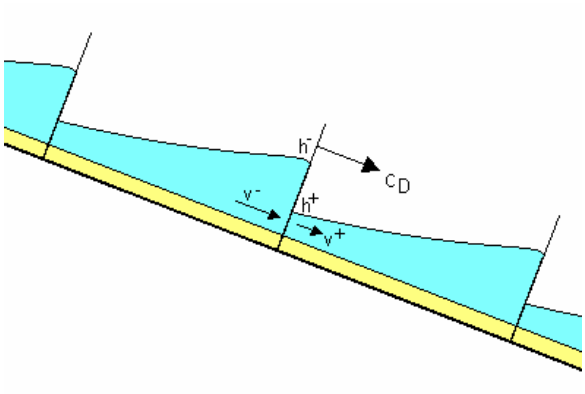

Figure 4-1Roll-waves after Dressler [2]

Roll-waves are observed in open-channel hydraulics and are stair-like structures that move down-stream (Figure 4-1). Roll-waves are a possibility in debris flows as well as is clearly seen in Figure 2-5. Similar structures are reported by Forterre & Pouliquen [3] in granular flows.

Dressler [2] has shown that in open channel hydraulics these roll waves cannot be described with patching of piece-wise continuous "Bresse profiles". He showed also that the dynamic stability of these roll waves is explained from the fact that the front $D(t)$ is a shock wave which moves with a constant celerity c_D. Ahead of the shock the flow is super-critical, whereas behind the shock it is sub-critical. It can be shown that in this case the particles move through the shock front, from the region of small flow-height to the region of big height.

5 Appendix I: The material time derivative

In the frame of the Eulerian description of the motion all quantities are seen as functions of the spatial co-ordinates of the material points at current time and of the time variable. For example in an 1D setting, the velocity of a particle P which at time t occupies the position x is given as a function of x and t,

$$v = v^E(x,t) \tag{4.1}$$

Where the superscript E is redundant and is put in order to remind that the description of the motion is an Eulerian one (cf. R.J. Roberts [6]).

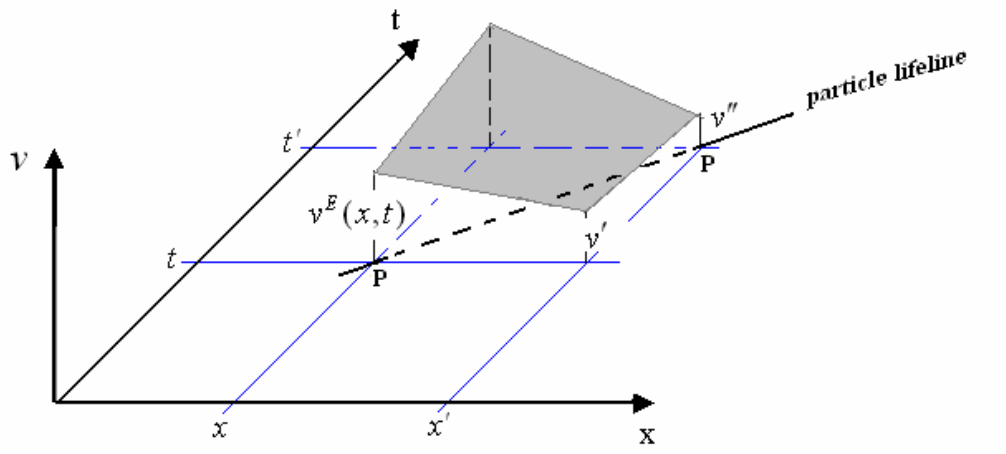

Figure 5-1: The Eulerian description of the velocity field in time-space and the computation of the "material" time derivative of the velocity.

At a following time instant, $t' = t + \Delta t$, the considered particle P has moved to a neighboring position, say, $x' = x + \Delta u$, the incremental displacement of the particle is given by the particle's velocity at the "event" (x,t) and the elapsed time interval:

$$\Delta u \approx v^E(x,t)\Delta t \tag{4.2}$$

With the velocity field given, eq.(4.1), the velocity of the considered particle P at this new position is,

$$v' = v^E(x',t') = v^E(x + \Delta x, t + \Delta t) \tag{4.3}$$

If we want to compute the acceleration $a = a^E(x,t)$ of the particle we have to compare the velocity $v = v^E(x,t)$ of the particle at its original position to its velocity at its new position, $v'' = v^E(x',t')$,

$$a \approx \frac{v'' - v}{\Delta t} \tag{4.4}$$

or according Figure 5-1,

$$a \approx \frac{1}{\Delta t}\left(\left(v' - v\right) + \left(v'' - v'\right)\right) \tag{4.5}$$

The first term in the parenthesis on the r.h.s. of eq. (4.5) is computed as follows:

$$v' - v = v^E(x + \Delta x, t) - v^E(x,t) \approx \frac{\partial v^E}{\partial x}\Delta x \tag{4.6}$$

and the second term as

$$\begin{aligned} v'' - v' &= v^E(x + \Delta x, t + \Delta t) - v^E(x + \Delta x, t) \\ &\approx v^E(x, t + \Delta t) - v^E(x,t) \approx \frac{\partial v^E}{\partial t}\Delta t \end{aligned} \tag{4.7}$$

Thus

$$a = \frac{\partial v^E}{\partial t} + \frac{\partial v^E}{\partial x} v^E \tag{4.8}$$

In fluid mechanics the above expression for the particle acceleration in an Eulerian description of the motion is called the *"material" time derivative* of the velocity field, because it accounts for the changes in the velocity as it is experienced by an observer who moves together with the particle (along the life-line of the particle). The material time derivative is denoted usually with a superimposed dot:

$$\dot{v} = \frac{\partial v^E}{\partial t} + v^E \frac{\partial v^E}{\partial x} \tag{4.9}$$

The material time derivative consists of the *local term*, $(\partial v / \partial t)$, and of the *convective term*, $v(\partial v / \partial x)$. The convective term is *non-linear*, since it consists of the product of the velocity and its spatial derivative. In solid mechanics applications the

convective term is usually negligible. In fluid mechanics and granular flow mechanics applications however convective terms are essential and cannot be neglected.

6 Appendix II: The limit equilibrium solutions for an infinite incline

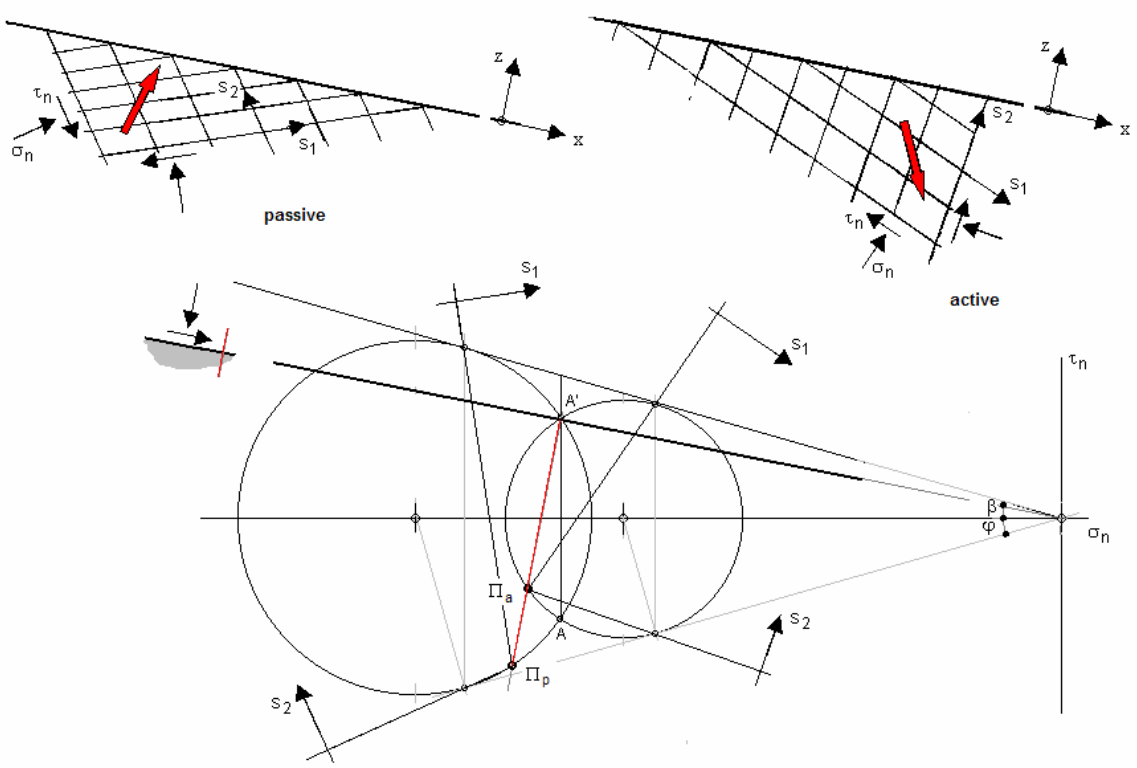

Figure 6-1: The infinite incline at limit equilibrium

We consider the case of an infinitely extending incline with the dip angle β of granular material at rest. The coordinate system (x, z), is chosen with axes parallel and normal to the free surface of the incline (Figure 6-1). We assume that all stress components are independent of the slope-parallel coordinate. In this case the local equilibrium equations become,

$$\frac{\partial \sigma_{zx}}{\partial z} + \rho g \sin\beta = 0 \Rightarrow \sigma_{zx} = \rho z \sin\beta(-z)$$
$$\frac{\partial \sigma_{zz}}{\partial z} - \rho g \cos\beta = 0 \Rightarrow \sigma_{zz} = \rho z \cos\beta \quad z \tag{5.1}$$

From the above expression it follows that along planes which are parallel to the free surface the stress ratio is constant,

$$\left|\frac{\sigma_{zx}}{\sigma_{zz}}\right| = \tan\beta \tag{5.2}$$

If we assume that the granular material is at limit equilibrium, then from the corresponding Mohr-circles of stresses we obtain two distinct solutions, the so-called "active" and "passive" case. The geometric construction of these solutions follows from the observation that the traction $(\sigma_{zz}, \sigma_{zx})$ acting on a plane $z = const.$ is mapped on the point A. Its mirror image A' and the related poles Π_a και Π_p lie on the same straight line.

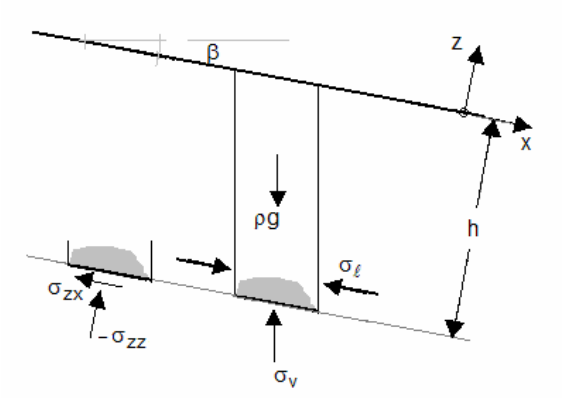

Figure 6-2: Stresses on a slice

From this geometric construction we get the following expressions for the vertical and the lateral stress, acting on the base of a slice, whose normal height is h (Taylor [10]),

$$\sigma_v = \rho g h$$

$$\frac{\sigma_{\ell,\min}}{\rho g h} = \frac{\rho g h}{\sigma_{\ell,\max}} = \Lambda \ , \ \Lambda = \frac{\cos\beta - \sqrt{\cos^2\beta - \cos^2\varphi}}{\cos\beta + \sqrt{\cos^2\beta - \cos^2\varphi}} \tag{5.3}$$

From this equation we can compute the lateral "earth-pressure" coefficient:

$$K_{p/a} = \frac{<\sigma_{xx}>}{<\sigma_{zz}>} = \tan^2\beta + \frac{1}{\cos^2\beta}\left(\frac{\cos\beta - \sqrt{\cos^2\beta - \cos^2\varphi}}{\cos\beta + \sqrt{\cos^2\beta - \cos^2\varphi}}\right)^{\pm 1} \tag{5.4}$$

or

$$K_{p/a} = 2\left(1 \pm \sqrt{1 - \frac{\cos^2\phi}{\cos^2\beta}}\right)\frac{1}{\cos^2\phi} - 1 \quad , \quad 0 \le \beta \le \phi \tag{5.5}$$

We emphasize that these earth-pressure formulae do not have meaning for a dip angle larger than the friction angle, and should not be applied to flowing granular sheets, where indeed $\beta > \phi$ holds.

In particular for a slope angle differing but little from the friction angle,

$$\beta = \phi - \delta \ , \ 0 \le \delta << 1 \tag{5.6}$$

we get

$$K_{p/a} = \frac{1 + \sin^2\varphi}{\cos^2\varphi} \pm O\left(\delta^{1/2}\right) \tag{5.7}$$

For almost horizontal slopes

$$\beta = \delta \ , \ 0 < \delta << 1 \tag{5.8}$$

we get the well-known expressions from Soil Mechanics

$$K_{p/a} = \frac{1 \pm \sin\phi}{1 \mp \sin\phi} \pm O\left(\delta^2\right) \approx \tan^2\left(45^\circ \pm \phi/2\right) \tag{5.9}$$

7 Appendix III: Shear flow of Bagnold frictional fluid

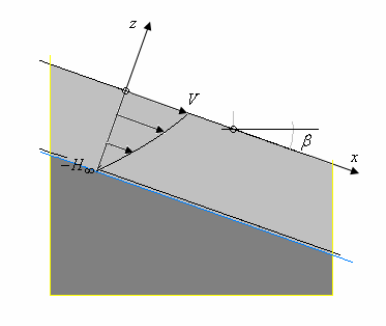

Figure 7-1: Shear layer forming on an inclined track

In order to get the flow-profile for a Bagnold-type frictional fluid we consider in a dynamic setting the governing equation (Figure 7-1),

$$\frac{\partial \tau}{\partial z} + \rho' g \sin\beta = \rho \frac{\partial v_x}{\partial t} \tag{6.1}$$

From eqs. (2.4) and (6.1) we get

$$\frac{3}{2} 2^{-3/2} c \left(\frac{\partial v}{\partial z} \right)^{1/2} \frac{\partial^2 v}{\partial z^2} + b = \frac{1}{g'} \frac{\partial v}{\partial t} \tag{6.2}$$

where the parameter c is given by eq. (2.17) and b is defined in eq. (2.23). The steady-state problem is described by the following o.d.e.,

$$2^{-3/2} \frac{c}{b} \left(\frac{\partial v}{\partial z} \right)^{1/2} \frac{\partial^2 v}{\partial z^2} + \frac{2}{3} = 0 \tag{6.3}$$

We introduce the following dimensionless variables (Figure 7-1),

$$z^* = \frac{z}{H_\infty} \quad , \quad v^* = \frac{v}{2V} \tag{6.4}$$

and with that eq. (6.3) becomes

$$\frac{c}{b} \left(\frac{V}{H_\infty} \right)^{3/2} \frac{1}{H_\infty} \left(\frac{\partial v^*}{\partial z^*} \right)^{1/2} \frac{\partial^2 v^*}{\partial z^{*2}} + \frac{2}{3} = 0 \tag{6.5}$$

We observe that in view of (2.22),

$$\left(\frac{V}{H_\infty}\right)^{3/2}\frac{1}{H_\infty}\frac{c}{b}=1 \tag{6.6}$$

Thus eq. becomes,

$$\left(\frac{\partial v^*}{\partial z^*}\right)^{1/2}\frac{\partial^2 v^*}{\partial z^{*2}}+\frac{2}{3}=0 \tag{6.7}$$

The general solution of eq. (6.7) is,

$$v^*=-\frac{3}{5}\left(c_1-z^*\right)^{5/3}+c_2 \tag{6.8}$$

First we impose the boundary condition at the bottom of the shear layer

$$for\quad z^*=-1:\quad v^*=0 \tag{6.9}$$

thus resulting to the following equation

$$c_2=\frac{3}{5}\left(1+c_1\right)^{5/3} \tag{6.10}$$

and with that

$$v^*=\frac{3}{5}\left(\left(1+c_1\right)^{5/3}-\left(-z^*+c_1\right)^{5/3}\right) \tag{6.11}$$

The boundary condition at the top of the shear layer is

$$for\quad z^*=0:\quad v^*=1 \tag{6.12}$$

thus yielding to the following equation

$$\left(1+c_1\right)^{5/3}-c_1^{5/3}-\frac{5}{3}=0\quad\Rightarrow\quad c_1=0.5142 \tag{6.13}$$

The corresponding velocity profile is depicted in Figure 7-2. One can see that it corresponds indeed to a shear-flow profile.

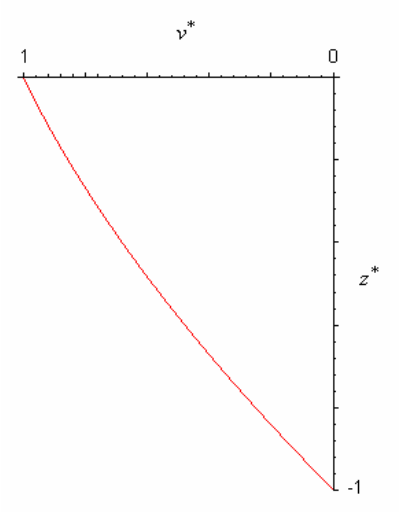

Figure 7-2: Velocity profile for a Bagnold fluid in steady shear

8 References

[1] Bagnold, R. A. (1954). Experiments on a gravity free dispersion of large solid spheres in a Newtonian Fluid under shear. Proceedings of Royal Society, London, A 225, 49–63.

[2] Dressler, R.F. (1949). Mathematical solution of the problem of roll-waves in inclined open channels. Communications on Pure and Applied Mathematics, 2, 149-194.

[3] Forterre, Y. and Pouliquen, O. (2003). Long surface wave instability in dense granular flows. J. Fluid Mech. 486, 21–50.

[4] Gray, J. M. N. T., Tai, Y.-C. and Noelle, S. (2003) Shock waves, dead-zones and particle-free regionsin rapid granular free surface flows. J. Fluid Mech. 491, 161–181.

[5] Quecedo, M., Pastor, M., Herreros, M.I., Merodo, J.A.F. (2004). Numerical modelling of the propagation of fast landslides using the finite element method. International Journal for Numerical Methods in Engineering 59 (12), 1633-1656

[6] R.J. Roberts, A One-Dimensional Introduction to Continuum Mechanics, World Scientific, 1994.

[7] Savage, S.B. and Hutter, K. (1989). The motion of a finite mass of granular material down a rough incline. J. Fluid Mech. 199, 177-215.

[8] Pouliquen, O. (1999). On the shape of granular fronts down rough inclined planes. Physics of Fluids, 11, 1956-1958

[9] Tai, Y. C., Noelle, S., Gray, J.M.N.T. and Hutter, K. (2001). Shock-Capturing and Front-Tracking Methods for Granular Avalanches, Journal of Computational Physics 175, 269–301

[10] D.W. Taylor, *Fundamentals of Soil Mechanics*, Wiley, p. 419ff, 1948.

[11] Vardoulakis, I. (2007). Basic Geodynamics of Landslides: I. The Dynamic Slip Circle Method, Lecture Notes LARAM School 2007.